Electrochemistry Communications 135 (2022) 107219

Contents lists available at ScienceDirect

Electrochemistry Communications

journal homepage: www.elsevier.com/locate/elecom

Full Communication

Recent developments in Pd-CeO_2 nano-composite electrocatalysts for anodic reactions in anion exchange membrane fuel cells

Hamish A. Miller [a,*], Marco Bellini [a], Dario R. Dekel [b,c], Francesco Vizza [a]

[a] Institute of Chemistry of Organometallic Compounds – National Research Council of Italy (ICCOM-CNR), Via Madonna del Piano 10, 50019 Sesto Fiorentino (Florence), Italy
[b] Wolfson Department of Chemical Engineering, Technion – Israel Institute of Technology, Haifa 3200003, Israel
[c] Nancy and Stephen Grand Technion Energy Program (GTEP), Technion – Israel Institute of Technology, Haifa 3200003, Israel

ARTICLE INFO

Keywords:
Palladium
CeO_2
Anion exchange membranes
Fuel cells
Anodic reactions

ABSTRACT

In 2016, for the first time a polymer electrolyte fuel cell free of Pt electrocatalysts was shown to deliver more than 0.5 W cm^{-2} of peak power density from H_2 and air (CO_2 free). This was achieved with a silver-based oxygen reduction (ORR) cathode and a Pd-CeO_2 hydrogen oxidation reaction (HOR) anodic electrocatalyst. The poor kinetics of the HOR under alkaline conditions is a considerable challenge to Anion Exchange Membrane Fuel Cell (AEMFC) development as high Pt loadings are still required to achieve reasonable performance. Previously, the ameliorative combination of Pd and CeO_2 nanocomposites has been exploited mostly in heterogeneous catalysis where the positive interaction is well documented. Carbon supported Pd-CeO_2 HOR catalysts have now been prepared by different synthetic techniques and employed in AEMFCs as alternative to Pt and PtRu standards. Important research has also been recently reported, delving into the origin of the HOR enhancement on Pd-CeO_2. Such work has highlighted the importance of the bifunctional mechanism of the HOR at high pHs. Carefully prepared nano-structures of Pd and CeO_2 that promote the formation of the Pd-O-Ce interface provide optimal binding of both H_{ad} and OH_{ad} species, aspects which are crucial for enhanced HOR kinetics. This review paper discusses the recent advances in Pd-CeO_2 electrocatalysts for AEMFC anodes.

1. Introduction

Cerium dioxide (CeO_2) is a technologically important material with a relatively high natural abundance in nature. It finds wide application as a "promoter" in three-way catalysts for the elimination of toxic auto-exhaust gases[1,2] and for the low-temperature water–gas shift (WGS) reaction. The wide range of catalytic applications of CeO_2 has been extensively reviewed recently.[1,3–5] The application of CeO_2 in low temperature electrocatalytic applications (fuel cells and electrolysis) is a small but growing field with its potential as catalyst or catalyst support yet to be fully determined.[6,7] One of the key catalytic functions of CeO_2 is the ability of Ce to switch between the Ce^{4+} and Ce^{3+} oxidation states, which allows the reversible addition and removal of oxygen, the so-called oxygen storage capacity.[8] This has allowed the use of non-stoichiometric CeO_2 nanoparticles as reactive oxygen species (ROS) scavenger in Nafion membranes.[9] Harmful HO• radicals can be scavenged by lattice oxygen vacancy sites, resulting in the concomitant oxidation of Ce3 + to Ce4 + . The Ce3+ (and hence vacancies) are then regenerated on the surface of the ceria nanoparticles under acidic conditions. Ce(OH)3 is the thermodynamically stable species of Pd-CeOx/C in a AEMFC anode (high pH) at OCV. However, as the anode is polarized quite significantly when operating at high current densities the electrode could reside near to the Ce4 + region and hence Ce + 3/Ce + 4 redox processes can become significantly involved in the HOR mechanism.[10] To overcome its inherent insulating capacity when used for electrocatalysis, CeO_2 is used in combination with conductive carbon and must be opportunely designed so that the two phases are chemically interfaced with overlapping orbitals, such that the conductivity of the carbon is partly transferred to the oxide through diffusion of freely moving electrons. In such cases, the resulting ternary composite relies on the CeO_2 phase to function as a promoter for the catalytically active site that is the metal nanoparticle. Engineering the structure of such ternary catalysts requires a high level of synthetic complexity, and in general, it is necessary to attain good dispersity of the transition metal species on the CeO_2, maximizing their net interfacial contact. This is especially true of the Pd-CeO_2-carbon class of hybrid materials that show remarkable enhancement of the alkaline hydrogen oxidation and alcohol oxidation reactions compared to benchmark Pt/C and Pd/C

* Corresponding author.

https://doi.org/10.1016/j.elecom.2022.107219

Available online 21 January 2022

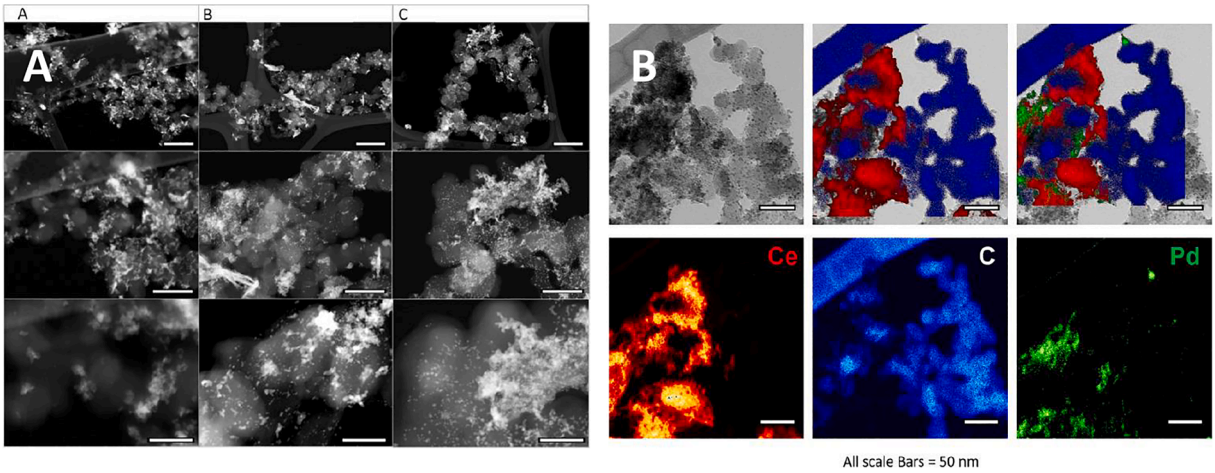

Fig. 1. Pd-CeO_2/C first reported in 2016 (A) Comparison between the three Pd loadings (A 6%, B 10% and C 20%) on CeO_2:C (50:50%) at three different magnifications: scale bar of the first line is 200 nm, middle line 100 nm and bottom line 50 nm. (B) STEM-EDX analysis of a representative portion of the 20 wt% Pd catalyst. Reprinted from ref. 20 with permission from Elsevier.

materials. Indeed, a recent LCA study highlights the environmental benefits of replacing Pt wth Pd-CeO_2 in fuel cells.[11] The recent acceleration in development of AEMFCs that operate with an alkaline environment has sparked renewed interest in the alkaline HOR and the challenge of overcoming sluggish HOR.[12–16] In this mini-review we highlight recent developments in the application of Pd-CeO_2-carbon type electrocatalysts applied in anion exchange membrane fuel cells (AEMFC) at the anode electrode interface where fuel oxidation takes place. This review concentrates on both hydrogen oxidation and also on alcohol oxidation and deals with the correlation between synthesis method, resulting nanostructure and the effect on catalytic activity. The bi-functional nature of HOR on Pd-CeO_2 composites is also discussed in light of recent DFT calculations.

2. Alkaline hydrogen oxidation reaction (HOR)

Currently, there are two principle theories proposed to describe the HOR mechanism under higher pHs.[17] The Hydrogen Binding Energy (HBE) theory and the bifunctional theory. The principle steps involved are:

$$\text{Tafel: } H_2 + 2^* \rightarrow 2H^* \quad (1)$$

$$\text{Heyrovsky: } H_2 + OH^- + * \rightarrow H^* + H_2O + e\text{-} \quad (2)$$

$$\text{Volmer: } H^* + OH\text{-} \rightarrow * + H_2O + e\text{-} \quad (3)$$

H_2 is oxidized to water molecules through Tafel-Volmer (1,3) or

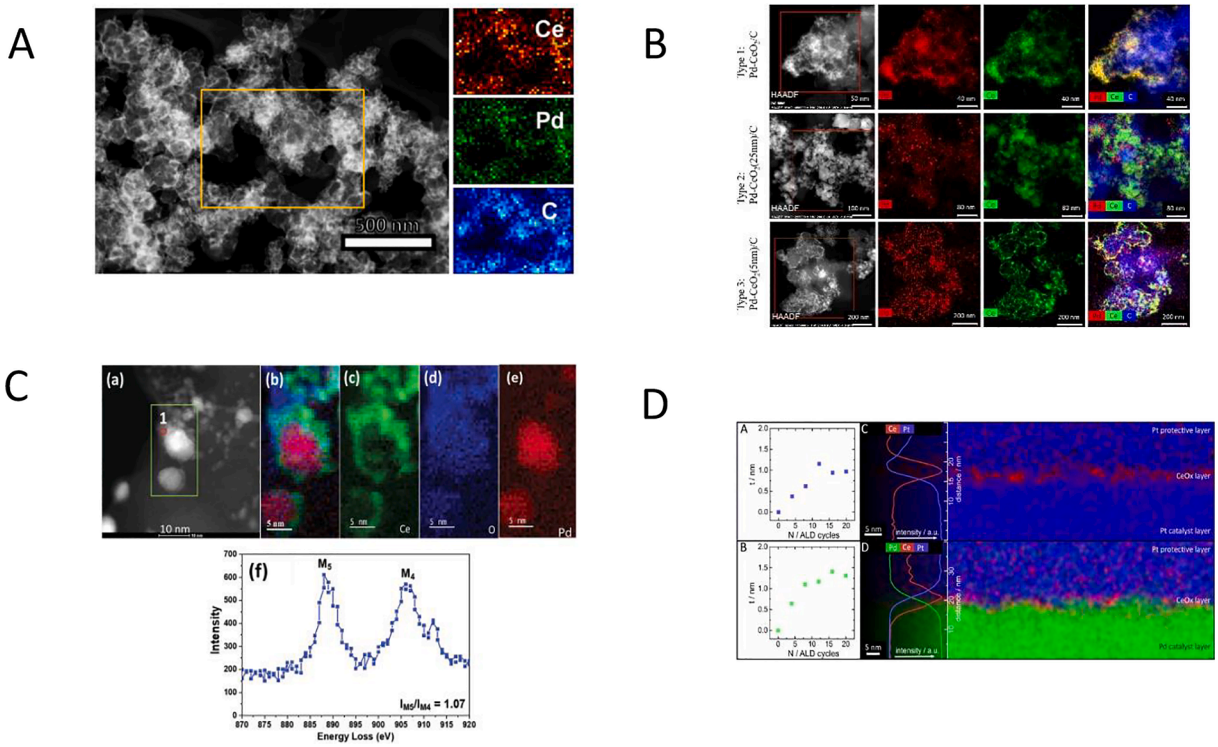

Fig. 2. Engineered Pd-CeO_2 nanostructures designed to enhance alkaline HOR activity. (A) Organometallic cerium precursor coated carbon (Reprinted with permission from ref.22. Copyright 2019 American Chemical Society), (B) flame-based reactive spray co-deposition of CeO_2 and Pd NPs Reprinted from ref. 23 with permission from Elsevier, (C) thin layers of ceria on surface of Pd nanoparticles [25]and (D) CeOx overlayers of different thicknesses on flat Pd surfaces by ALD [26].

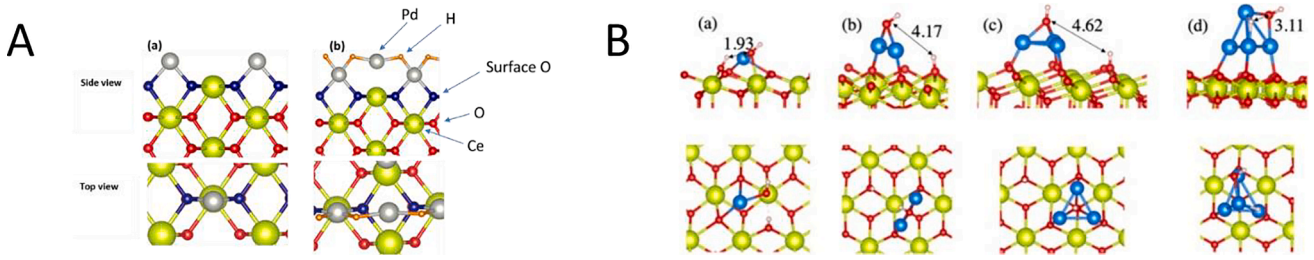

Fig. 3. (A) (a) Adsorption of Pd on bridge site between the O atoms of the CeO_2 (1 1 0) (b) Adsorption of H in between the Pd atoms. Green, grey and orange color ball represents Ce, Pd and H atoms, respectively. O atoms are in red and blue color, in order to distinguish the surface O atoms (blue) from other O atoms (red) in the slab. Reprinted with permission from ref.22. Copyright 2019 American Chemical Society. (B) Stable adsorption configuration of the reactant species (H* and OH*) on a Pd–CeO_2 substrate considered for understanding the Volmer mechanism. The numbers correspond to the distances between H and O–(OH) species in Å. Reprinted with permission from ref.28. Copyright 2021 American Chemical Society.

Heyrovsky-Volmer (2,3) mechanisms. The HBE theory involves H_{ad} initially desorbed as a proton which then reacts with OH^- to generate water. If this mechanism predominates at high pH, then the hydrogen binding energy (HBE) would be the sole determining factor for HOR kinetics. The second mechanism includes OH^- that is also adsorbed on the surface of the metal catalyst ($M-OH_{ad}$), where the H_{ad} and OH_{ad} subsequently react to form water. With this mechanism, both HBE and the OHBE (OH_{ad} binding energy) are important for determining HOR activity.[18] HOR kinetics on Pt catalyst surfaces in the alkaline environment of AEMFCs are 2–3 orders of magnitude slower than in acidic Proton Exchange Membrane Fuel Cells (PEMFC). Lower cost and more sustainable alternatives to Pt with enhanced HOR activity are required for pushing AEMFC technology forward. Such an example was provided by Miller et al who demonstrated enhancements in the alkaline HOR using Pd-CeO_2 interactions on a Vulcan carbon support.[19,20] The CeO_2 plays a key role in the HOR through rapid saturation with OH^- ions in alkaline media and spill over of OH^- to the supported Pd nanoparticles. Evidence was also found for a weakening of the Pd-H binding energy due to the presence of CeO_2. The combination of enhanced OH transfer and Pd-H bond weakening supports the bi-functional mechanism where both the Pd-OH and Pd-H bonding are descriptors that account for the alkaline HOR.

The first synthesis procedure involves the formation of a mixed CeO_2 and carbon phase through the precipitation of CeOx with alkali followed by heat treatment (still air atmosphere, 250 °C, 2 h) that forms a heterogeneous material with distinctive CeO_2 structures agglomerated onto the carbon particles (Fig. 1A).[19] STEM analysis clearly shows this heterogeneous structure of 50:50 wt% composite and the preferential deposition of Pd onto the ceria phase. Such a structure however does not favour exploitation of the Pd-CeO_2-C interface with the deposited Pd collecting mainly on the CeO_2 portions but with a significant amount on the bare carbon surface (no Pd-CeO_2). Add to this the Pd supported on large CeO_2 structures separated from the carbon networks where electronic resistance will be high (unutilised Pd-CeO_2). This explains the relatively poor performance of 20% Pd compared to the 10% Pd material.[20] Indeed, STEM-EDX analysis of the surface of the 20% Pd material clearly shows these two aspects of the catalyst (Fig. 1B).

Researchers have since then developed new synthesis techniques to help probe and maximise the Pd-CeO_2-C interfacial interactions. Each synthesis method is designed to obtain a certain structure and investigate the roll-on effect on activity. In a first strategy, researchers tackled the first step of CeO_2 deposition onto Vulcan Carbon.[21,22] Exploiting Vulcan carbon activated with oxygen surface group interaction with an organometallic Cerium alkoxyl compound formed a well dispersed uniform layer of cerium on Vulcan. Careful decomposition to CeO_2 yielded a homogeneous thin layer of amorphous CeO_2 (Fig. 2A). This allowed the deposition of Pd to form a highly dispersed Pd phase. XAS analysis shows 100% oxidised single Pd atoms coordinated to surface O atoms of CeO_2.[22]

Yu and co-workers prepared three types of Pd–CeO_2/C catalysts synthesized by a single flame-based reactive spray deposition technology (RSDT) process, where the HOR activity correlated to increased Pd–CeO_2 interfacial contact.[23] Both Pd and Ce precursors were sprayed together and a homogeneous distribution of small Pd and CeO_2 nanoparticles (both around 5 nm) was obtained leading to higher HOR activity. This study confirmed the direct relationship between the increased amount of PdO to Pd ratio (82%) and enhanced HOR activity (Fig. 2B).

In another recent work, Yarmiayev et al. reported enhanced HOR activity of Pd through CeO_2 surface doping.[24] Based on the electrochemical surface area estimation, the authors claimed that the improved activity is due to a vertical growth of CeO_2 islands onto the Pd surface that enhances the Pd-CeO_2 interface area. The HOR activity with the highest CeO_2-doped material was improved by 50–100 times as compared to pristine Pd and was mainly attributed to the change in HBE and the oxophilicity of CeO_2.

Creating thin layers of ceria onto Pd nanoparticles is a strategy exploited also by Singh and co-workers.[25] Tris(cyclopentadienyl) cerium(III) was used as a precursor for the addition of CeOx using sequential CSR cycles. This addition of an organometallic precursor allowed the controlled addition of CeOx to the Pd NP surfaces (Fig. 2C). The 0.38 ratio of Ce to Pd provided the best HOR activity and the best yet reported for Pd-ceria catalysts (55 mA mg_{Pd}^{-1}). The highest Pd(IV)/Pd (0) ratio of 50% present in carbon supported Pd@CeO_x(0.38) results from partial charge transfer from metallic Pd to CeOx.

In a recent study, a model of a quasi-2D buried electrocatalytic interface system with a well-controlled overlayer thickness was prepared in order to study both activity and stability of Pd-CeO_2 systems simultaneously on a fundamental level.[26] This model simplifies the complex 3D structure of real Pd-CeOx/C catalysts. The system was realized by using atomic layer deposition (ALD) to deposit CeOx overlayers of different thicknesses onto flat Pd surfaces, thus forming CeOx@Pd interfaces (Fig. 2D). A layer of 5.5 ± 0.5 nm CeO_2 for Pd–Ce_{20} was obtained. The addition of CeOx to Pd increases its catalytic activity toward the HOR and at same time, causes a 10-fold decrease in Pd dissolution, which suggests that the ceria stabilizes the Pd against dissolution in the alkaline medium.

In a completely different synthetic process, CeO_2@Pd HOR catalyst has been prepared using a new materials methodology of molecular doping of metals. The Pd matrix, which encages the ceria nanoparticles, is prepared in foam architecture, to ensure easy molecular diffusion.[27] The authors claimed to observed experimental evidence of the weakening of Pd–H bond in the CeO_2@Pd composites, relative to pure (undoped) Pd catalysts. Gas diffusion electrodes based on the entrapped CeO_2@Pd catalysts demonstrated one order of magnitude higher activity than pure Pd analog in the HOR reaction in an alkaline medium.

3. DFT *ab initio* studies

The HOR mechanism on Pd-ceria anode catalysts has been explored

Table 1
Summary of AEMFC performance data with Pd-CeO_2 HOR catalysts.

Anode Pd loading mg cm^{-2}	Cathode	Metal loading mg cm^{-2}	T_{cell} °C	H_2 Flow (SLPM)	O_2 Flow (SLPM)	@ 600 mV W cm^{-2} (A cm^{-2})	Peak power W cm^{-2} (A cm^{-2} at peak)	Membrane Ionomer	Ref.
0.25	Pt/C	0.40	80	1	2	1.25 (2.0)	2.0 (5.0)	HDPE-AEM (ETFE powder)	[29]
0.25	Pd/C	0.25	80	1	2	0.7 (1.1)	1.3 (3.9)	HDPE-AEM (ETFE powder)	[29]
0.25	Ag-CoPc/C	0.75 Ag	80	1	2	0.45 (0.9)	1 (3.6)	HDPE-AEM (ETFE powder)	[29]
0.25	Fe/C	0.03	60	1	2	0.43 (0.71)	0.96 (2.7)	HDPE-AEM (ETFE powder)	[29]
0.60	Pt/C	0.60	80	2	1	0.50 (0.8)	0.7 (1.5)	TPN (FLN)	[30]
0.55	Pt/C	0.70	60	1	1	0.45 (0.9)	0.62 (1.4)	ETFE-BTMA Fumatech powder	[25]
0.5	Co3O4	3	70	1	0.5	0.3 (0.5)	0.39 (0.9)	AT-1 aQAPS-S14	[31]
0.42	PdCu	0.58 (Pd)	70	1	1	0.8 (1.3)	1.0 (2.4)	ETFE-BTMA (ETFE powder)	[32]
0.25	Pt	0.4	80	1	2	0.75 (2)	1.4 (3.3)	LDPE-AEM (ETFE powder)	[22]
0.3	Ag/C	3	73	0.2	1	0.3 (0.5)	0.5 (1.5)	–	[19]

using ab-initio studies. In a preliminary work DFT studies concentrated on the study of a 5 atomic layer surface of CeO_2 (1 1 0) with Pd atoms adsorbed on bridge sites between O atoms of CeO_2.[22] The HBE of Pd-CeO_2 was calculated and compared to Pd. As shown in Fig. 3A, H prefers to adsorb in the bridge site between the Pd atoms on a monolayer. The HBE weakens on the Pd-CeO_2 surface relative to Pd suggesting the enhancement in HOR activity is due to this effect. Thicker layers of Pd behave like bulk Pd suggesting that very small Pd NPs or single atoms will produce higher HOR activity an observation supported by experimental data.

In a more complex study by Alpay and co-workers, the HOR activity for Pd-ceria surfaces was studied using Ab initio DFT calculations probing the interplay between the important adsorbed species, H, OH and H_2O on model surfaces (Fig. 3B).[28] The Tafel and Volmer reactions were investigated. The study concluded that a surface with 10 wt % Pd on a CeO_2 surface has enhanced HOR activity due to a delicate balance between the H and OH interactions with the Pd-CeO_2 support with a low H-BE and a moderate OH-BE combined with maximized charge donation of Pd to surroundings. This bi-functional mechanism where both H and OH binding energies are activity descriptors is supported by experimental data that has shown 10 wt% Pd as optimized loading.[20]

4. Performance in AEMFCs

Pd-CeO_2/C catalysts synthesised by different methodologies have been incorporated in MEAs with anion exchange ionomers and AEMs and combined with various cathode catalysts and tested in H_2/O_2 fuel cells. A summary of the reported power densities and test conditions is shown in Table 1.

From the data reported in Table 1 it is clear that Pd-CeO_2 produces very high power densities in AEMFCs. The highest reported peak power density of 2 W cm^{-2} was obtained at 80 °C with a Pt/C cathode and HDPE-AEM combined with a powder ETFE ionomer and is certainly on a par with PtRu/C and Pt/C standards. It is also clear that the cell performance is governed by the cathode catalyst employed. Under the same conditions a Fe/C cathode produced only circa 1 W cm^{-2}. Indeed, it is clear that Pd-CeO_2 anodes combined with PGM based cathodes produce higher peak power densities and higher power densities at higher cell potential (0.6 V) than when Pd-CeO_2 is coupled with non Pt cathodes.

5. Alkaline alcohol oxidation

Prof. P.K. Shen first reported the electrochemical oxidation of methanol, ethanol, glycerol and ethylene glycol in alkaline media on Pt and Pd catalysts using a novel mixed CeO_2 and carbon support. [33–36] Later Vizza and co-workers confirmed that the presence of CeO_2 promotes the formation of Pd-OH_{ad} species at lower potentials and this

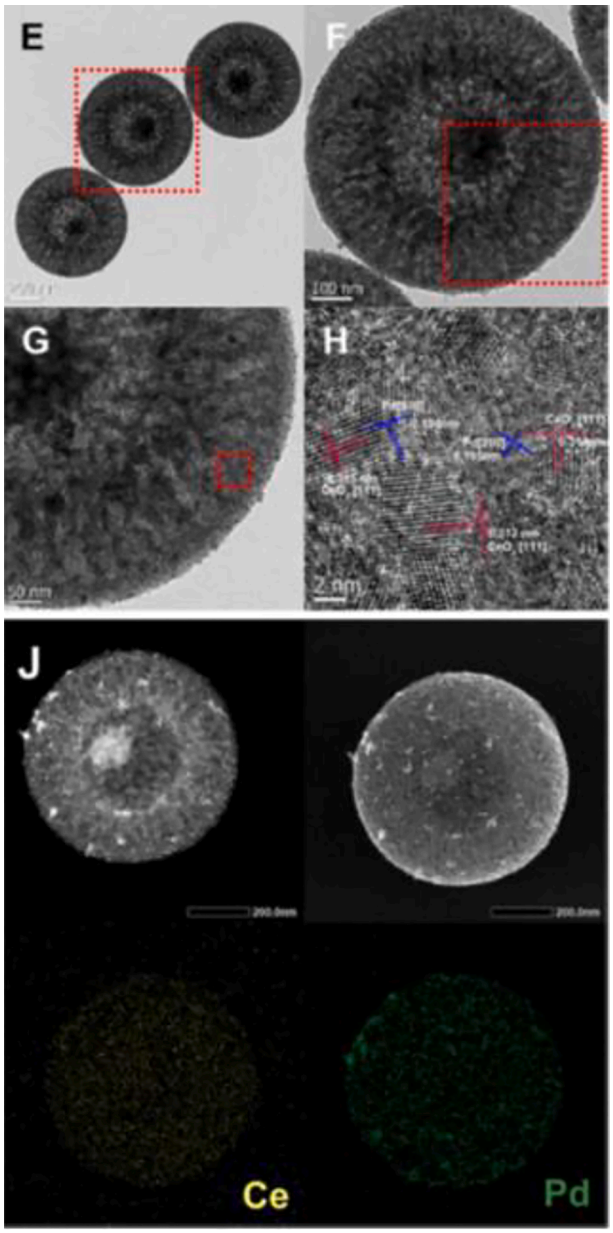

Fig. 4. TEM images of Pd-CeO_2/NMCS (E – H) catalysts with different magnifications. HAADF-STEM, secondary electron image, and elemental mapping of Pd-CeO_2/NMCS (J). Adapted from ref. 43.

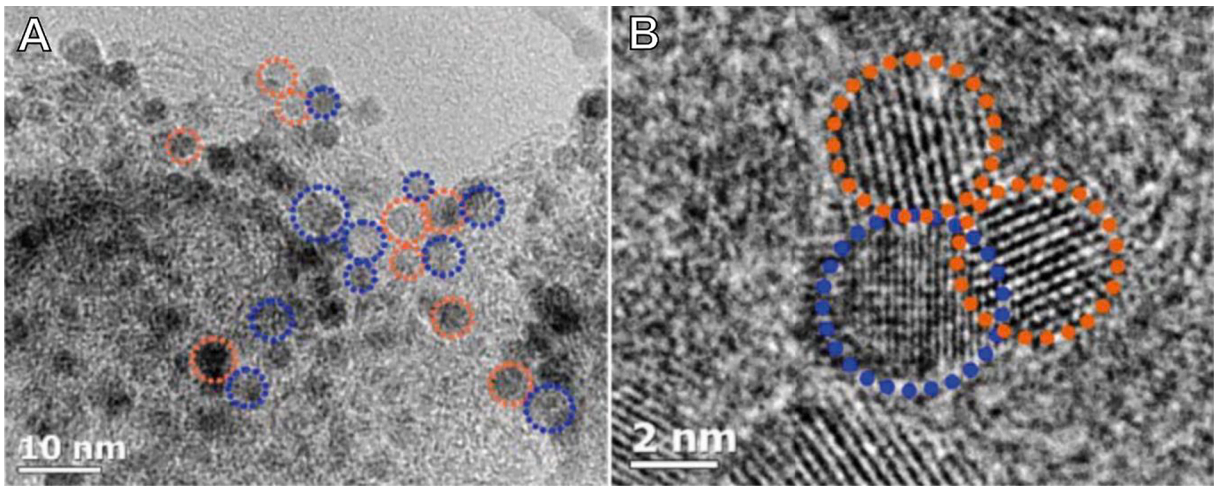

Fig. 5. (A) TEM and (B) HRTEM images of Pd/Co-CeO_2. Orange circles marks Co-CeO_2 dots and blue circles the Pd nanoparticles. Figure adapted from ref. 48 with permission from RSC.

effect doubled the energy efficiency of direct ethanol fuel cells operating in alkaline media.[37,38] The ameliorative effect of Pd-CeO_2 interactions was extended to other alcohols in subsequent studies including formate,[39] methanol,[40] glycerol,[40] ethylene glycol,[40] 1,2-propandiol,[40] 1,3-propanediol,[41] 1,4-butandiol,[40] allyl alcohol.[42] Engineering the catalyst architecture plays as much of a crucial role in the oxidation of alcohol fuels as with H_2. Wu and co-workers to this end synthesized core–shell mesoporous nitrogen-doped mesoporous carbon spheres (NMCS) decorated with Pd-ceria nanoparticles.[43] The spheres are based on a carbon core decorated with a mesoporous coralline-like shell with high surface area (489 $m^2\ g^{-1}$) and a mean diameter of 480 nm. Ceria dots of 3.5 nm were grown inside the pores by thermal decomposition of cerium (IV) ammonium nitrate and acted as precipitating sites for Pd nanoparticles (ca. 13 nm) (Fig. 4). The resulting $Pd_{(20\%)}$-$CeO_{2(20\%)}$/NMCS electrocatalyst showed a six times higher activity for methanol oxidation compared to a state of the art PtRu/C catalyst.

Yavari et al directly incorporated Pd nanoparticles in a ceria sponge obtained by a solution combustion synthesis.[44] The resulting carbon free catalyst is a porous ceria powder decorated with Pd nanoparticles both inside and over the pores. The BET surface area of 47.72 m^2g^{-1} improved the Pd nanoparticle dispersion, improving the catalyst activity for alkaline methanol oxidation. Chen et al. developed an inverse CeO_2/Pd nanostructured catalyst supported on carbon for formate oxidation.[45] Thin ceria islands were generated on Pd NPs with a $Pd_{72}Ce_{28}$ alloy at the interface. A peak current density produced by formate oxidation is 3.8 times that of Pd/C. Modifying the CeO_2 geometry is another strategy for tuning catalyst activity. Rodríguez-Varela supported 5.5 nm Pd NPs on a mixture of Vulcan and ceria nanorods ($CeO_{2\text{-}NR}$).[46] The synergistic effect between Pd and $CeO_{2\text{-}NR}$ was improved and a mass activity of 697 mA mg_{Pd}^{-1} for ethanol oxidation was obtained. Annealing the ceria nanorods at 400 °C ($CeO_{2\text{-}NR4}$) reduced the crystallite size improving the subsequent Pd dispersion.[47] The very small 1.1 nm Pd nanoparticles improved catalyst mass activity for ethanol oxidation. Moreover, the catalyst showed high activity for other C1, C2 and C3 alcohols. Hybrid catalytic systems based on metal doped CeO_2 nanostructures can improve ceria dispersion compared to traditional catalysts, which have significant CeO_2 aggregation. High ceria dispersion also improves catalyst oxophylicity. Wu and Liu prepared small monodispersed cobalt doped CeO_2 dots of 3.6 nm by a thermal decomposition process on carbon that was then combined with Pd for methanol and ethanol electrooxidation.[48] An intimate contact between Pd and Co-CeO_2 dots was obtained thanks to the anchoring effect of ceria dots for Pd nanoparticles (Fig. 5). The resulting catalyst electrochemical activity was improved compared to a state of the art Pd-CeO_2/C catalyst.

6. Summary and perspectives

In this review we discuss recent developments in Pd-CeO_2-C catalysts for the anodic reactions of AEMFCs (HOR and AOR). The search for more sustainable alternatives to Pt is complicated by the slow kinetics of the HOR at higher alkalinities. It has now been shown that Pd-CeO_2 interactions improve the HOR kinetics through a bifunctional mechanism that involves a weakening of the Pd-H_{ad} binding energy and an optimisation of Pd-OH_{ad} binding. Electron transfer from Pd to CeO_2 is also an important factor as shown through *ab initio* modelling. Pd-CeO_2-C materials synthesised to maximise the interfacial contact between the three components have a high proportion of oxidised Pd atoms coordinated directly to the O atoms of the CeO_2 surface. The activity in AEMFCs is comparable to Pt and PtRu standards with power densities up to 2 W cm^{-2}. Evidence of improved *in operando* stability of Pd-CeO_2-C relative to Pd/C has been provided. Future developments of this new class of anode catalyst must involve reduction of the total electrode Pd loadings to less than 0.125 mg cm^{-2} to be coupled with non PGM cathodes (2025 target Anion Exchange Membrane Workshop 2019). We believe that single Pd atom active sites embedded in the CeO_2 surface should be prepared to this end.

CRediT authorship contribution statement

Hamish A. Miller: Conceptualization, Writing – original draft, Writing – review & editing. **Marco Bellini:** Writing – original draft. **Dario R. Dekel:** Writing – original draft. **Francesco Vizza:** Writing – original draft, Funding acquisition.

Declaration of Competing Interest

The authors declare that they have no known competing financial interests or personal relationships that could have appeared to influence the work reported in this paper.

Acknowledgements

We acknowledge funding of a PRIN 2017 Project funded by the Italian Ministry MUR Italy (Grant No. 2017YH9MRK). We also acknowledge the Italian Ministry MISE for the FISR 2019 project AMPERE (FISR2019_01294).). This work was partially funded by the Nancy & Stephen Grand Technion Energy Program (GTEP); by the Israel

Science Foundation (ISF) [grant No. 1481/17], and by the Mauerberger Foundation Fund (MFF).

References

[1] M. Melchionna, et al., Synthesis and properties of cerium oxide-based materials, Metal Oxides (2020) 13.
[2] A. Trovarelli, et al., Catal Today 50 (1999) 353.
[3] T. Montini, et al., Chem Rev 116 (2016) 5987.
[4] G. Korotcenkov, Cerium Oxide (CeO_2): Synthesis, Properties and Applications Preface to the series, Metal Oxides, (2020) Xv-Xvii.
[5] E. Aneggi, et al., Catalytic applications of cerium dioxide, Metal Oxides (2020) 45.
[6] M. Melchionna, et al., Mater Today Adv 6 (2020), 100050.
[7] M. Melchionna, P. Fornasiero, Mater Today 17 (2014) 349.
[8] C.W. Sun, et al., Energ Environ Sci 5 (2012) 8475.
[9] P. Trogadas, et al., Acs Appl Mater Inter, 4 (2012), 4 (10), 5098.
[10] P. Abellan, et al., Rsc Adv 7 (2017) 3831.
[11] S. Minelli, et al., Hydrogen 2 (2021) 246.
[12] S. Gottesfeld, et al., J Power Sources 375 (2018) 170.
[13] D.R. Dekel, et al., J Power Sources 375 (2018) 158.
[14] J.R. Varcoe, et al., Energ Environ Sci 7 (2014) 3135.
[15] E.S. Davydova, et al., Acs Catal 8 (2018) 6665.
[16] D.R. Dekel, Ecs Transactions 50 (2013) 2051.
[17] L.X. Su, et l., J Energy Chem, 66 (2022) 107.
[18] D.R. Dekel, Curr Opin Electroche 12 (2018) 182.
[19] H.A. Miller, et al., Angew Chem Int Edit 55 (2016) 6004.
[20] H.A. Miller, et al., Nano Energy 33 (2017) 293.
[21] A. Lenarda, et al., Inorg Chim Acta 470 (2018) 213.
[22] M. Bellini, et al., ACS Appl Energ Mater 2 (2019) 4999.
[23] H.R. Yu, et al., Nano Energy 57 (2019) 820.
[24] V. Yarmiayev, et al., J Electrochem Soc 166 (2019) F3234.
[25] R.K. Singh, et al., Adv Funct Mater 30 (2020) 2002087.
[26] F.D. Speck, et al., 32 (2020) 7716.
[27] N. Ralbag, et al., J Electrochem Soc 167 (2020).
[28] S. Sahoo, et al., ACS Catal 11 (2021) 2561.
[29] H.A. Miller, et al., ACS Appl Energ Mater 3 (2020) 10209.
[30] S. Maurya, et al., ACS Catal 8 (2018) 9429.
[31] V.M. Truong, et al., Energies 13 (2020) 582.
[32] T.J.P. Omasta, et al., J Electrochem Soc 165 (5) (2018) J3039.
[33] P.K. Shen, C.W. Xu, Electrochem Commun 8 (2006) 184.
[34] C.W. Xu, et al., Electrochim Acta 51 (2005) 1031.
[35] C.W. Xu, P.K. Shen, Chem Commun (2004) 2238.
[36] C.W. Xu, et al., Electrochim Acta 53 (2008) 2610.
[37] V. Bambagioni, et al., Chemsuschem 5 (2012) 1266.
[38] L.Q. Wang, et al., Chemcatchem 7 (2015) 2214.
[39] H.A. Miller, et al., Energies 11 (2018) 369.
[40] M. Bellini, et al., Inorg Chim Acta 518 (2021).
[41] J. Mahmoudian, et al., Acs Sustain Chem Eng 5 (2017) 6090.
[42] M.V. Pagliaro, et al., Inorg Chim Acta 525 (2021).
[43] Q. Tan, et al., ACS Catal 9 (2019) 6362.
[44] Z. Yavari, et al., Korean J Chem Eng 37 (2020) 1669.
[45] Q. Tang, et al., J Mater Chem A 7 (2019) 22996.
[46] P.C. Melendez-Gonzalez, et al., Chemistryselect 5 (2020) 14032.
[47] J.E. Solis-Tobias, et al., Int J Hydrogen Energ 44 (2019) 12415.
[48] Q. Tan, et al., Nanoscale 9 (2017) 12565.